manuscript.

[1]A typical example is that of an antiferromagnetic insulator-to-paramagnetic metal transition; see, for example, D. B. McWhan, T. M. Rice, and J. P. Remeika, Phys. Rev. Lett. 23, 1384 (1969).

[2]The possibility of having an exchange interaction between the interstitial atom and remaining atomic sites can be incorporated easily in this model and would lead to a different magnetic state in the disordered phase. For the sake of simplicity in this paper we will assume that no coupling of this nature exists.

[3]If x is the number of interstitials available per atom, then $Q = x + 1$.

[4]$n_i > Q^{-1}$ would imply the formation of a superlattice of correlated interstitials, i.e., the onset of a new type of order.

[5]By melting we mean a first-order transition into a quasicrystalline disordered state which characterizes the liquid state. See, for example, J. Frenkel, *Kinetic Theory of Liquids* (Dover, New York, 1955).

[6]B. A. Huberman and W. Streifer, to be published.

[7]C. Guillaud, J. Phys. Radium 12, 223 (1951); R. R. Heikes, Phys. Rev. 99, 446 (1955).

[8]The melting point in MnBi is of a peritectic character and takes place at 446°C.

[9]B. W. Roberts, Phys. Rev. 104, 607 (1956).

[10]T. Chen, private communication.

Molecular-Dynamics Investigation of Structural Phase Transitions

T. Schneider and E. Stoll
IBM Zurich Research Laboratory, 8803 Rüschlikon, Switzerland
(Received 9 July 1973)

We report on a molecular-dynamics study of a two-dimensional model system which is expected to exhibit antiferrodistortive structural phase transitions. The estimated values for the critical exponents β and γ are close to those of the two-dimensional Ising model. The origin of a central peak in the dynamic form factor is attributed to the formation and the dynamics of clusters.

Experimental and theoretical studies have emphasized the need of an anharmonic treatment of lattice dynamics in systems undergoing a structural phase transition.[1-4] The molecular-dynamics technique is a powerful way of examining the static and dynamic properties associated with these transitions, since anharmonicity is treated without approximation.[5]

In this note we report molecular-dynamics results performed on a two-dimensional model system which is expected to exhibit antiferrodistortive structural phase transitions. There exist two extreme cases: the order-disorder and displacive transitions.[1,6]

A prominent example of an antiferrodistortive displacive transition is $SrTiO_3$. A feature of this transition is that it exhibits nonclassical fluctuations as demonstrated by paramagnetic resonance studies.[7,8] A second attractive feature is the appearance of a central peak in addition to the conventional soft-mode resonance in the dynamic form factor of the density fluctuations at the R corner ($T \geq T_c$) and the Γ point ($T \leq T_c$) of the Brillouin zone, respectively.[9,10]

The unexpected appearance of the central peak gave rise to many theoretical speculations on the nature of this phenomenon.[11-15] From the presently available neutron-scattering data, however, the origin of the observed peak cannot be elucidated because of resolution limitations. This open question was one of the compelling reasons for making a molecular-dynamics study.

A model Hamiltonian, covering the whole range from the order-disorder limit to the displacive limit, reads[1,6]

$$\mathcal{H} = \sum_{l,\kappa} \left[\tfrac{1}{2} (\vec{P}_\kappa^{\,l})^2 + \tfrac{1}{2} A (\vec{U}_\kappa^{\,l})^2 + \tfrac{1}{4} B (\vec{U}_\kappa^{\,l})^4 \right] + C \sum_{l,\kappa} \sum_{l',\kappa'} \vec{U}_\kappa^{\,l} \cdot \vec{M}_{\kappa\kappa'}^{\,ll'} \vec{U}_{\kappa'}^{\,l'} \cdot \vec{M}_{\kappa\kappa'}^{\,ll'} . \quad (1)$$

$\vec{P}_\kappa^{\,l}$ is the momentum of the κth particle in the lth unit cell and $\vec{U}_\kappa^{\,l} = \vec{R}_\kappa^{\,l} - \vec{R}_{0\kappa}^{\,l}$ denotes the corresponding displacement from the reference position $\vec{R}_{0\kappa}^{\,l}$. The unit vector $\vec{M}_{\kappa\kappa'}^{\,ll'}$ equals $(\vec{R}_{0\kappa}^{\,l} - \vec{R}_{0\kappa'}^{\,l'}) / |\vec{R}_{0\kappa}^{\,l} - \vec{R}_{0\kappa'}^{\,l'}|$ for nearest neighbors and is zero otherwise. The arrangement of the particles and the constraints subjected to the displacements are shown in Fig. 1 for a two-dimensional system. These constraints imply that we consider only an antiferrodistortive transition,

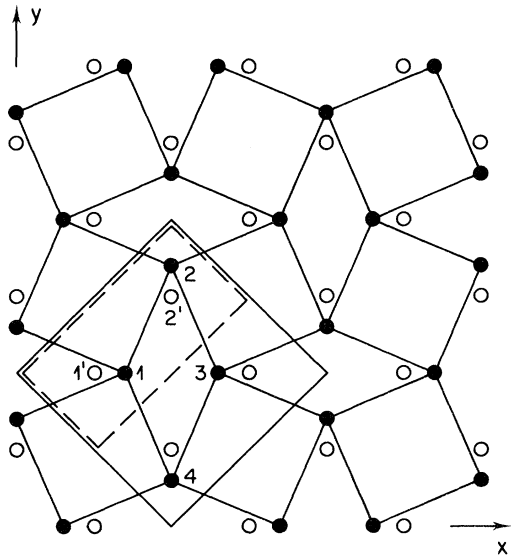

FIG. 1. Arrangement of the particles in the low- and high-temperature phases. Open circles form the reference lattice which is equivalent to that of the high-temperature phase, with atoms 1′ and 2′ per unit cell. Closed circles denote the positions of the particles in the low-temperature phase with four atoms per unit cell. Particle 1′ displaces only in the x direction, and particle 2′ in the y direction, whereas particles 1 and 3 displace in the x direction, and 2 and 4 in the y direction.

corresponding to the motions of the oxygen atoms of $SrTiO_3$ in the a-b plane.[3,7] The order parameter for such a two-dimensional system is given by the scalar

$$\langle U\rangle = (4N)^{-1}\sum_l \langle U_{1x}{}^l + U_{2y}{}^l - U_{3x}{}^l - U_{4y}{}^l\rangle. \quad (2)$$

The model parameters have been chosen as follows: for model I,

$$A=-1,\quad B=\tfrac{1}{3},\quad C=-1,\quad a=4\langle U\rangle|_{T=0}=12; \quad (3)$$

for model II,

$$A=\tfrac{1}{2},\quad B=\tfrac{1}{3},\quad C=-1,\quad a=5.66\langle U\rangle|_{T=0}=12; \quad (4)$$

a is the lattice constant. All units are set equal to 1 and as a consequence all quantities are dimensionless. According to the Hartree approximation,[1,6] model I undergoes an antiferrodistortive order-disorder and model II an antiferrodistortive displacive transition.

The dynamics of this system is assumed to evolve according to Newton's equations associated with Hamiltonian (1). We consider a system of 40×40 high-temperature unit cells (Fig. 1), subjected to periodic boundary conditions. The particles are then allowed to move and their canonical variables are calculated according to a set of difference equations with a time increment. This set of difference equations approximates the set of Newton's equations. Explicit details of programming and the form chosen for the difference equations are given in the papers of Rahman[16] and Verlet.[17] For our purpose, however, it was more convenient to keep the temperature constant. This can be achieved by adjusting the instantaneous values of the velocities after any time increment in such a way that T remains fixed. In this procedure equilibrium is reached, while the instantaneous value of the order parameter, for example, fluctuates about a mean value. Using the equilibrium data saved one might then calculate space-time correlation functions, related to the linear response of the system, and time averages. The limitations of this technique as a tool to investigate phase transitions are similar to those of the Monte Carlo method. They have been discussed in that context extensively.[18]

Our data for the order parameter [Eq. (2)] taken at different temperatures indicate that in the corresponding infinite system (model I) T_c is close to 5.35 and $\beta\approx\frac{1}{8}$. In model II we found $T_c \approx 2.13$ and again $\beta\approx\frac{1}{8}$. As expected, then, the divergence of the staggered isothermal susceptibility was found to be consistent with $\gamma\approx\gamma'=\frac{7}{4}$, the value of the two-dimensional Ising model. The Hartree approximation[1,6] leads to $\beta=\frac{1}{2}$, $\gamma=1$, $T_c=9$ (model I) and $T_c=4.5$ (model II).

An interesting observation was made by analyzing the temporal development of the system. In fact, it turned out that the system forms clusters, representing connected cells whose instantaneous local order parameter $\frac{1}{2}[U_{1x}{}^l(t)+U_{2y}{}^l(t)]$ or $-\frac{1}{2}\times[U_{3x}{}^l(t)+U_{4y}{}^l(t)]$ has a sign opposite to that expected from $\langle U\rangle_{T=0}$, so that

$$\operatorname{sgn}\left\{\begin{array}{l}\frac{1}{2}[U_{1x}{}^l(t)+U_{2y}{}^l(t)]\\ -\frac{1}{2}[U_{3x}{}^l(t)+U_{4y}{}^l(t)]\end{array}\right\}\neq \operatorname{sgn}\langle U\rangle_{T=0}. \quad (5)$$

Figure 2 shows snapshots of cluster configurations in model II at various temperatures. It is seen that the clusters increase by approaching $T_c\approx 2.13$ from above or below. Similar behavior was found in model I.

The occurrence of these clusters has a marked effect on the dynamics of the system. In fact, a given particle not only takes part in the conventional vibrations but it is also tied to the cluster dynamics, which becomes slower and slower by

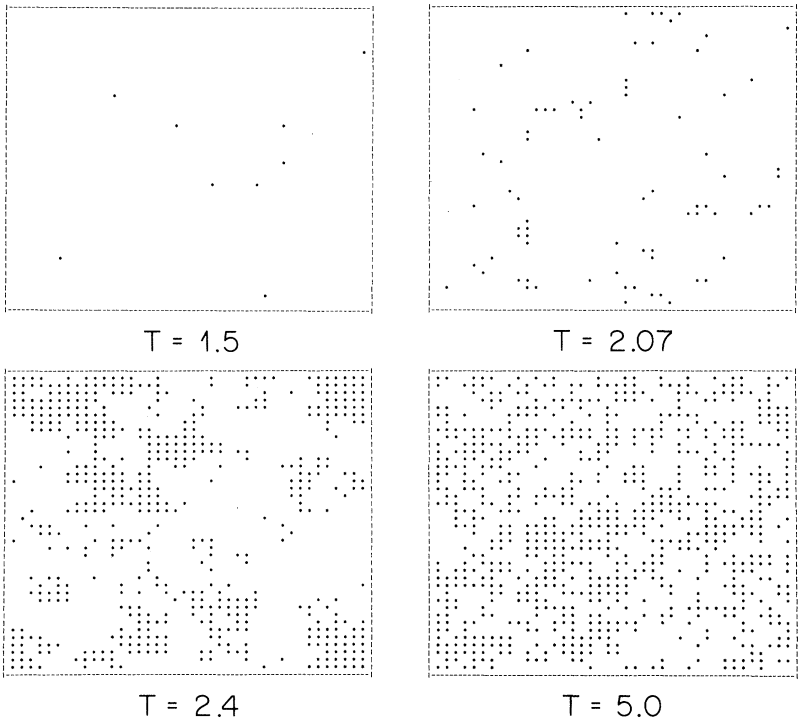

FIG. 2. Snapshots of instantaneous cluster configurations in model II ($T_c \approx 2.13$). Points denote cells with local order parameter $\frac{1}{2}[U_{1x}^{l}(t) + U_{2y}^{l}(t)]$ or $-\frac{1}{2}[U_{3x}^{l}(t) + U_{4y}^{l}(t)]$ opposite to $\langle U \rangle_{T=0}$, Eq. (5).

approaching T_c. As a consequence, by approaching T_c one expects an additional low-frequency spectrum in the spectral density of the time-dependent correlation functions of the density, the order parameter, and the potential energy. This view has been confirmed by our simulations. In Figs. 3 and 4, we show as an example the frequency dependence of the spectral density

$$\hat{S}_{\rho\rho}(\vec{k},\omega) = \frac{S_{\rho\rho}(\vec{k},\omega)}{S_{\rho\rho}(\vec{k},t=0) - |\langle \rho(\vec{k}) \rangle|^2}, \tag{6}$$

at various temperatures for models I (Fig. 3) and II (Fig. 4) at $\vec{k} = (\pi/a)\{3,1\}$. The spectral density or the dynamic form factor is defined by

$$S_{\rho\rho}(\vec{k},\omega) = \int_{-\infty}^{+\infty} dt\, e^{-i\omega t} S_{\rho\rho}(\vec{k},t),$$
$$S_{\rho\rho}(\vec{k},t) = \langle \rho(-\vec{k},0)\rho(\vec{k},t) \rangle, \tag{7}$$

$$\rho(\vec{k},t) = (1/\sqrt{N}) \sum_{l,\kappa} \exp[-i\vec{k}\cdot\vec{R}_{\kappa}^{\,l}(t)]. \tag{8}$$

$\vec{R}_{\kappa}^{\,l}$ denotes the position vectors of the particles. From Fig. 3 it is seen that by approaching T_c from above or below a central peak appears as such. Below T_c, the resonances of the conventional soft mode appear at $\omega \approx 1.4$ ($T = 4$) and $\omega \approx 1.2$ ($T = 5$). At $T = 5$, however, the central peak dominates the spectrum and the resonance due to the soft transverse mode is very weak. Above $T_c \approx 5.35$, the $T = 6$ spectrum is again dominated by the central peak. The conventional soft-mode resonance appears again at $T = 10$ ($\omega \approx 0.9$) and the central peak is considerably weaker. It is no longer visible at $T = 20$.

In model II (Fig. 4) the low-temperature spectrum [Fig. 4(b)] is dominated by the conventional soft-mode resonance, marked by arrows. For $T \gtrsim 1.5$, however, we observe the appearance of a low-frequency spectrum, which explains the decreasing intensity of the resonance due to the conventional soft mode. At $T = 2.05$ the low-frequency spectrum is dominated by an intense peak at $\omega = 0.12$, appearing at $T = 2.07$ as a central peak. This low-frequency spectrum must be attributed to the cluster dynamics, becoming slower and slower by approaching T_c. Consequently, close enough to T_c, this low-frequency spectrum may either go over into a central peak or will appear as such as a result of resolution limitations. Above T_c, the temperature dependence of the spectrum is qualitatively similar to that below T_c [Fig. 4(b)]. The low-frequency peak, however, is more pronounced and appears at $T = 2.4$ as a central peak. Additional spectral densities

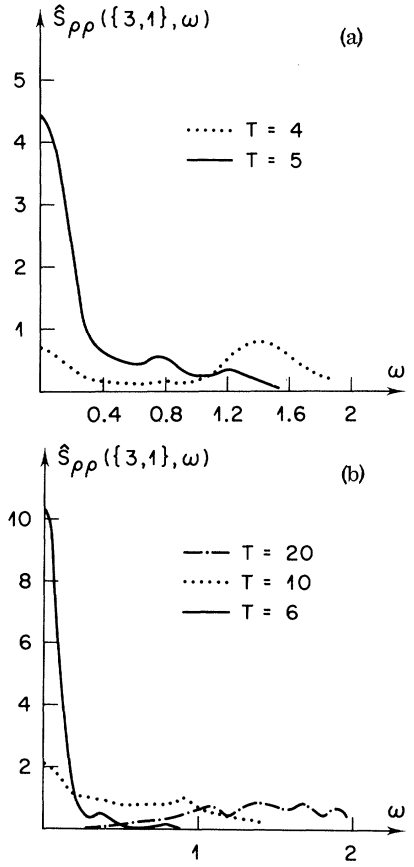

FIG. 3. Frequency dependence of the dynamic form factor $\hat{S}_{\rho\rho}(\vec{k},\omega)$ in model I at $\vec{k}=(\pi/a)\{3,1\}$. (a) $T=4$ and $T=5$; (b) $T=6$, $T=10$, and $T=20$.

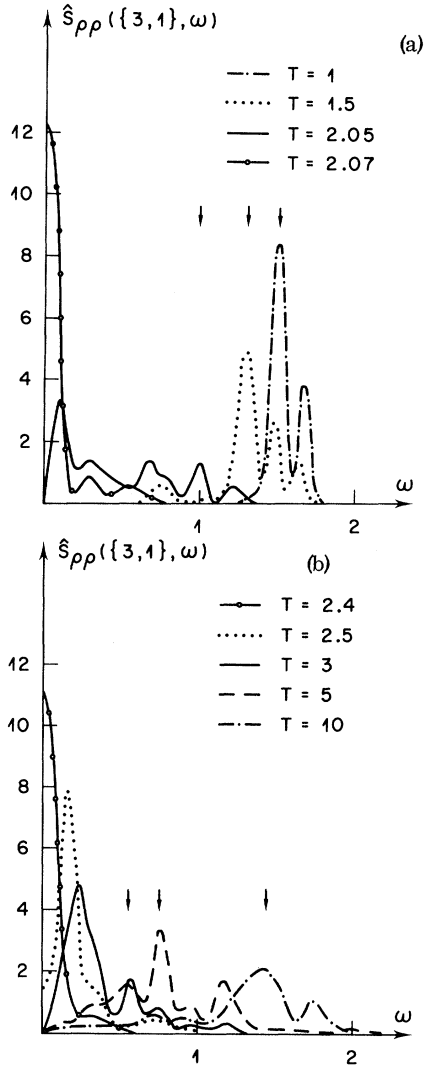

FIG. 4. Frequency dependence of the dynamic form factor $\hat{S}_{\rho\rho}(\vec{k},\omega)$ in model II (displacive model) at $\vec{k}=(\pi/a)\{3,1\}$. The arrows mark the peaks due to the conventional soft mode. (a) $T=1$, $T=1.5$, $T=2.05$, and $T=2.07$; (b) $T=2.4$, $T=2.5$, $T=3$, $T=5$, and $T=10$.

[Eq. (6)] have been calculated at $(\pi/a)\{1,1\}$ and $(\pi/a)\{2,0\}$, where the conventional soft mode is not expected to appear. Here we find well-defined phonon resonances, rather unaffected by the phase transition.

To summarize, we have shown that the critical dynamics of antiferrodistortive phase transitions is associated with the appearance of a central peak in the dynamic form factor $S_{\rho\rho}(\vec{k},\omega)$. The resonance of the conventional soft mode, however, becomes weaker by approaching T_c and no longer visible close to T_c. Moreover, our results suggest that this central peak is due to the formation of clusters and their dynamics. This mechanism has been neglected so far in the microscopic treatments.[4,11,13,15] The appearance of the central peak was found to be distinctly different in the displacive and disorder cases. There, the cluster dynamics were, as the appearance of the central peak revealed, mainly relaxational. In the displacive regime, however, the "extra" low-frequency response was not centered at $\omega=0$, except very near to T_c. This prediction could be verified by means of high-resolution inelastic neutron-scattering measurements.

We acknowledge stimulating discussions with K. A. Müller, P. Heller, C. P. Enz, N. Szabo, and P. F. Meier.

[1]See the various contributions, in *Proceedings of the NATO Advanced Study Institute on Structural Phase Transitions and Soft Modes, Geilo, Norway, 1971*, edited by E. J. Samuelsen, E. Anderson, and J. Feder (Universitetsforlaget, Oslo, Norway, 1972).

[2]P. A. Fleury, Comments Solid State Phys. 4, 149, 167 (1972).
[3]E. Pytte, Comments Solid State Phys. 5, 41, 57 (1973).
[4]Papers and references cited in Proceedings of the NATO Advanced Study Institute on Anharmonic Lattices, Structural Transitions and Melting, Geilo, Norway, 24 April–1 May 1973 (to be published).
[5]J. M. Dickey and A. Paskin, Phys. Rev. 188, 1407 (1969).
[6]H. Thomas, in Ref. 1, p. 15
[7]K. A. Müller and W. Berlinger, Phys. Rev. Lett. 26, 13 (1971).
[8]Th. von Waldkirch, K. A. Müller, and W. Berlinger, Phys. Rev. B 7, 1052 (1973).
[9]T. Riste, E. J. Samuelson, K. Otnes, and J. Feder, Solid State Commun. 9, 1455 (1971).
[10]S. M. Shapiro, J. D. Axe, G. Shirane, and T. Riste, Phys. Rev. B 6, 4332 (1972).
[11]C. P. Enz, Phys. Rev. B 6, 4695 (1972).
[12]F. Schwabl, Phys. Rev. Lett. 28, 500 (1972).
[13]R. Silberglitt, Solid State Commun. 11, 247 (1972).
[14]T. Schneider, Phys. Rev. B 7, 201 (1973).
[15]P. Meier, to be published.
[16]A. Rahman, Phys. Rev. 136, A405 (1964).
[17]L. Verlet, Phys. Rev. 159, 98 (1967).
[18]T. Schneider, E. Stoll, and K. Binder, Phys. Rev. B (to be published).

Absolute Cross Sections in ^{2}H- and ^{3}He-Induced Breakup Reactions

T. K. Lim
Department of Physics and Atmospheric Science, Drexel University, Philadelphia, Pennsylvania 19104
(Received 6 September 1973)

The absolute magnitudes and shapes of the cross sections of a number of ^{2}H- and ^{3}He-induced quasifree scattering processes are correctly predicted by the use of Eckart cluster-model wave functions for the light nuclei involved and a simple, but physically plausible, modification of the Rogers-Saylor attenuation model.

Quasifree scattering (QFS) in multiparticle reactions has been the subject of recent detailed study, both experimentally and theoretically.[1-5] In the analysis of data,[2,3,5] it appears that the plane-wave impulse approximation (PWIA) and the cluster-model approximation applied to such quasifree knockout reactions, $A(a,ab)B$, can be quite successful in predicting the general shape of the coincidence cross section. However, it has been found in each QFS where the cluster probability is well known, as in reactions involving $1s$-shell nuclei, that the PWIA curve is a little too broad, and a normalization factor is required to derive absolute fits to the data. It has also been determined that this factor is energy dependent.[1,3]

In the absence of a rigorous theory, similar to the Faddeev theory in three-particle problems, considerable theoretical interest has centered on removing, or deriving from some suitable model, this normalization factor, thus resuscitating PWIA as a viable instrument for QFS analysis. For example, Duck, Valkovic, and Phillips[2] utilize a large phenomenological off-shell correction to produce absolute magnitude and shape fits to the coincidence cross section of coplanar ^{2}H$(d,dp)n$ at 12.5 MeV. Also, Bonbright *et al.*[4] have shown that a smooth cutoff parameter in the Hulthén deuteron function, which varies with energy, is able to fulfill the same purpose.

In this work, I show that such deficiencies in PWIA analyses of recently studied ^{2}H- and ^{3}He-induced QFS processes can be removed by the use of Eckart cluster-model wave functions for the light nuclei[6] and a simple, but physically plausible, modification of the Rogers-Saylor attenuation model.[7] In the original model, the theoretical expression for the coincidence cross section to be compared with experiment is the usual PWIA expression multiplied by an attenuation factor. This factor is defined, for example, in $(p,2p)$ QFS as

$$T(\sigma_T) = \int \psi^*(\vec{r}) \exp(-\sigma_T/4\pi r^2)\psi(\vec{r})\, d^3r, \qquad (1)$$

where ψ is the cluster function representing the relative function of either final-state proton with respect to the spectator nucleus, while σ_T is the sum of experimental total cross sections of both protons on the spectator at the corresponding final-state energies. Physically, T represents the probability of transmission of the two protons after QFS into detectors located at the QFS kinematic region. Haracz and Lim[8] have shown that in symmetric, coplanar $(p,2p)$ reactions on ^{2}H, ^{3}He, and ^{4}He, Eckart wave functions and this attenuation factor can lead to excellent shape and